

An Improved Experimental Limit on the Electric Dipole Moment of the Neutron

C.A. Baker,¹ D.D. Doyle,² P. Geltenbort,³ K. Green,^{1,2} M.G.D. van der Grinten,^{1,2} P.G. Harris,² P. Iaydjiev*,¹ S.N. Ivanov†,¹ D.J.R. May,² J.M. Pendlebury,² J.D. Richardson,² D. Shiers,² and K.F. Smith²

¹*Rutherford Appleton Laboratory, Chilton, Didcot, Oxon OX11 0QX, UK*

²*University of Sussex, Falmer, Brighton BN1 9QH, UK*

³*Institut Laue-Langevin, BP 156, F-38042 Grenoble Cedex 9, France*

(Dated: July 22, 2019)

An experimental search for an electric-dipole moment (EDM) of the neutron has been carried out at the Institut Laue-Langevin (ILL), Grenoble. Spurious signals from magnetic-field fluctuations were reduced to insignificance by the use of a cohabiting atomic-mercury magnetometer. Systematic uncertainties, including geometric-phase-induced false EDMs, have been carefully studied. Two independent approaches to the analysis have been adopted. The overall results may be interpreted as an upper limit on the absolute value of the neutron EDM of $|d_n| < 3.0 \times 10^{-26} e \text{ cm}$ (90% CL).

PACS numbers: 13.40.Em, 07.55.Ge, 11.30.Er, 14.20.Dh

I. INTRODUCTION

In order for particles to have electric dipole moments, the forces concerned in their structure must violate both parity (P) and time reversal (T) symmetries. Although P violation is maximal in the weak interaction, T (and hence CP) violation is a rare phenomenon, the origins of which are not yet understood. Extensions to the Standard Model, such as additional Higgs fields, right-handed currents or supersymmetric partners typically give rise to neutron EDM (nEDM) contributions which are of order 10^{-25} to $10^{-27} e \text{ cm}$ [1, 2, 3, 4]; dipole moments of this size might also come from CP violation in QCD [5]. Experimental measurements of particle EDMs [6, 7, 8], and in particular that of the neutron, are providing some of the strongest additional constraints on these theories [9, 10].

II. EDM MEASUREMENT TECHNIQUE

This nEDM experiment, and the performance of its cohabiting mercury magnetometer, have been discussed in earlier publications [11, 12]. The measurement was made with ultracold neutrons (UCNs) stored in a trap permeated by uniform **E**- and **B**-fields. This adds terms $-\mu_n \cdot \mathbf{B}$ and $-\mathbf{d}_n \cdot \mathbf{E}$ to the Hamiltonian determining the states of the neutron. Given parallel **E** and **B** fields, the Larmor frequency $\nu_{\uparrow\uparrow}$ with which the neutron spin polarization precesses about the field direction is

$$h\nu_{\uparrow\uparrow} = |2\mu_n B + 2d_n E|. \quad (1)$$

For antiparallel fields, $h\nu_{\uparrow\downarrow} = |2\mu_n B - 2d_n E|$. Thus the goal was to measure any shift in the transition frequency

ν as an applied **E** field alternated between being parallel and then antiparallel to **B**.

A schematic of the apparatus is shown in Figure 1. The UCNs were prepared in a spin-polarized state by transmission through a thin, magnetized iron foil, and entered a 21-liter trap within a $1 \mu\text{T}$ uniform vertical magnetic field **B**₀. Approximately 20 s were needed to fill the trap with neutrons, after which the entrance door was closed pneumatically. The electric field, of approximately 10 kV/cm, was generated by applying high voltage to the electrode that constituted the roof of the trap, while keeping the floor electrode grounded.

The transition frequency ν of the neutrons was measured using the Ramsey separated oscillatory field magnetic resonance method. During the storage period, the neutrons interacted coherently with two 2 s intervals of oscillating magnetic field having a chosen frequency close to the Larmor frequency. The two intervals were separated by a period $T = 130$ s of free precession. The last step was to count the number of neutrons N_{\uparrow} and N_{\downarrow} that finished in each of the two polarization states. This was achieved by opening the entrance door to the trap, and allowing the neutrons to fall down onto the polarizing foil, which then acted as a spin analyzer. Only those in the initial spin state could pass through to the detector, which was a proportional counter in which neutrons were detected via the reaction $n + {}^3\text{He} \rightarrow {}^3\text{H} + p$. During one half of the counting period, an r.f. magnetic field was applied in the region above the polarizing foil; this flipped the spins of the neutrons, thereby also allowing those in the opposite spin state to be counted. In a data-taking run the batches were cycled continuously for 1-2 days. Periodically, after a preset number (typically 16) of batches, the direction of **E** was reversed. Each batch yielded about 15,000 UCN counts.

The magnetometer used the precession frequency of atoms of ¹⁹⁹Hg (with 3×10^{10} atoms/cm³) stored simultaneously in the same trap as the neutrons; the EDM of the ¹⁹⁹Hg atom was known to be very small [6]. A linear fit of the ratio R of neutron to mercury-atom precession frequencies as a function of the applied electric field yields

*On leave from Institute of Nuclear Research and Nuclear Energy, Sofia, Bulgaria

†On leave from Petersburg Nuclear Physics Institute, Russia

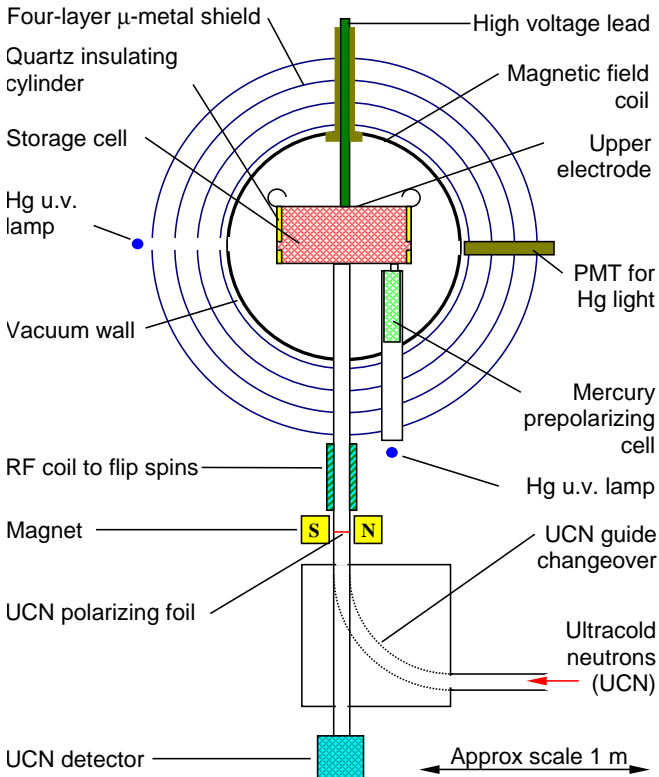


FIG. 1: (Color online) The neutron EDM experimental apparatus

a slope that is, in principle, directly proportional to the neutron EDM.

III. GEOMETRIC-PHASE EFFECTS

It has been shown [13] that a geometric phase arising from vertical (i.e. axial) gradients $\partial B_z / \partial z$ in the applied magnetic field induces false EDM signals in systems of stored particles. Because the center of gravity of the neutrons is $\Delta h = 0.28$ cm lower than the center of gravity of the mercury atoms, a vertical gradient shifts the Larmor frequencies of the two species slightly differently, allowing the value of the gradient in the trap to be deduced from the quantity

$$R_a = \left| \frac{\omega_n}{\omega_{\text{Hg}}} \cdot \frac{\gamma_{\text{Hg}}}{\gamma_n} \right|. \quad (2)$$

In this experiment, the geometric-phase effect acts most strongly upon the mercury atoms. Application of the mercury data to correct for magnetic field fluctuations then creates an apparent false neutron EDM of

$$d_{nf} = \pm \frac{\hbar}{8} \cdot |\gamma_n \gamma_{\text{Hg}}| \cdot \frac{R^2 B_{0z}}{\Delta h c^2} \cdot (R_a - 1), \quad (3)$$

where R is the radius of the trap and the + sign corresponds to \mathbf{B}_0 downwards. Figure 2 shows the measured

EDM as a function of $R_a - 1$ for each of the two directions of the applied magnetic field. The lines shown represent a least-squares fit ($\chi^2/\nu = 1.18$) to all of the data, in which the two intercepts and a common absolute value of the gradient are free parameters. The expected (from Eq. 3) absolute value $m = (1.57 \pm 0.08) \times 10^{-26}$ e cm/ppm of the line gradients is consistent (within 1.3σ) with the value of $(1.90 \pm 0.25) \times 10^{-26}$ e cm/ppm found by a fit to the data. The uncertainty in the expected gradient arises from a number of small effects: Δh has a 4% uncertainty; the presence of helium buffer gas, the door cavity, and the grooves that locate the trap walls all act to reduce the mean free path slightly, and hence [13, 14] to reduce the geometric-phase-induced EDM signal; and the neutrons' own geometric-phase signal increases the slope slightly, as does an enhancement [15] due to the dipole-like shape of the field from the trim coils that were used to apply magnetic field gradients.

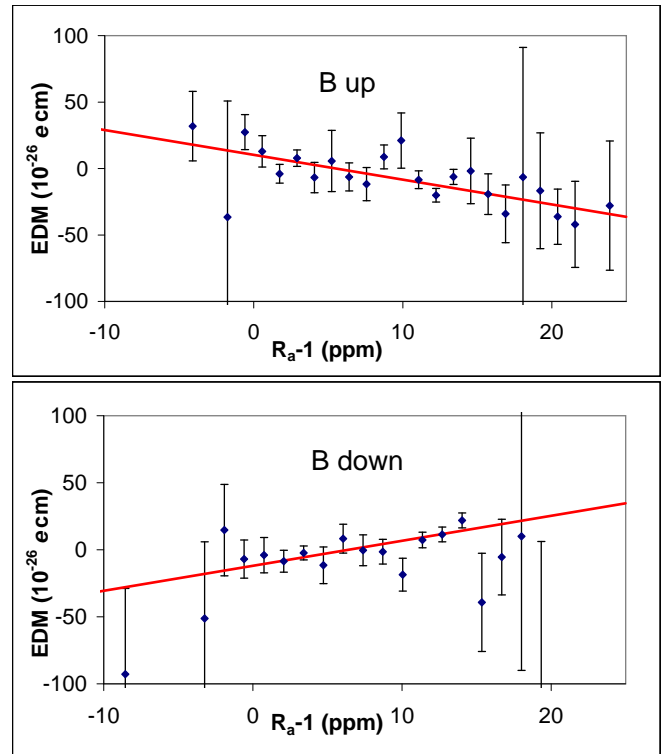


FIG. 2: (Color online) Measured EDM as a function of the relative frequency shift of neutrons and mercury. For clarity, data are binned.

Geometric-phase effects arising from uniform gradients in B_z can be eliminated by using the crossing point of the lines in Figure 2 (or equivalently by using the average of a suitably balanced data set). This is not the case in other situations, where changes in R_a and d_{nf} are not in the same ratio.

For both directions of B_z , gradients in horizontal fields B_{xy} without 2D divergence have the effect of increasing

the frequency ratio R_a quadratically [13] without creating any geometric-phase EDM. They can thus shift the lines of Figure 2 rightwards, without changing the EDM value at the intersection. If, however, the B_{xy} fields change strength when the main magnetic field is reversed, the lines of Figure 2 shift by different amounts, thus introducing a shift in the intersection value of the EDM.

Local magnetic-dipole fields can also induce geometric-phase false EDM signals d_{dip} . Studies [15] have shown that these signals are enhanced beyond the expectation, from Eq. 3, of a shift d_{nf} proportional to the volume-averaged gradient. The net effect of a given dipole is therefore to shift the lines of Figure 2 vertically by the residual amount $d_s = d_{dip} - d_{nf}$.

The trap used in the EDM measurements has a small cavity in the lower electrode, 4 cm deep and 6.8 cm in diameter at the base, just above the entrance door. Vertical magnetic field gradients here (due, for example, to magnetisation of the door, dipoles in the vicinity of the door cavity, or thermoelectric currents in the door mechanism) would be important because they can change the volume-averaged $\partial B_z / \partial z$ while (via Eq. 3) contributing almost nothing to the geometric-phase EDM because of the small radius of the door cavity. R_a would be shifted in opposite directions for the two polarities of \mathbf{B}_0 , thus generating a finite net shift in the EDM result. Flux-gate magnetometer scans of the storage volume revealed no magnetic anomalies ≥ 1 nT, but contaminants below this level, or fields arising from thermoelectric currents within the door mechanism as it operates in vacuum, cannot be ruled out.

IV. ANALYSES

Two independent approaches were adopted in studying these data. In the first, more straightforward, analysis, the two overall average $R_a - 1$ values after cuts were almost identical, with approximately equal amounts of data in each field direction. A simple weighted average of the data was then used as an estimator of the EDM. No attempt was made to compensate for other potential systematic biases: instead, a systematic uncertainty adequate to cover such biases was associated with the result. The value obtained in this manner was

$$d_n = (-0.2 \pm 1.6 \text{ (stat)}) \times 10^{-26} \text{ e cm} \quad (\chi^2/\nu = 1.24),$$

with an additional uniformly distributed systematic uncertainty of $\pm 1.2 \times 10^{-26}$ e cm allocated to it in order to accommodate any shifts arising from the effects listed in Table 1 and discussed in more detail below. The resulting distribution of possible values implies an upper limit on the absolute value of the neutron EDM of 2.9×10^{-26} e cm (90% CL).

The second analysis began with the crossing point value $d_n = (-0.55 \pm 1.51) \times 10^{-26}$ e cm (which includes a light shift correction, discussed below) of the fitted

lines in Figure 2, and then used complementary measurements to attempt to correct for systematic biases caused by dipolar non-uniformities in \mathbf{B}_0 . Precession-frequency measurements within the B field were made using separate but similar traps, with the same entrance door and with a variable-height roof so that known gradients $\partial B_z / \partial z$ could be set up. This revealed the value quoted above of $\Delta h = (0.28 \pm 0.01)$ cm for the displacement between the centers of mass of the neutrons and the mercury, in good agreement with an independent calculation of the number density distribution over the 12 cm bottle height of the UCNs after storage.

One variable-height bottle was of a smaller radius (18.5 cm) than the main data-taking bottle (23.5 cm). It also had a door cavity of depth 6 cm instead of 4 cm. The effects of any dipole field in the door cavity were therefore amplified. For a series of bottle heights H , a gradient-compensated reference value of $R_a - 1$ for which the mercury frequency was identical for both height H and height $H/2$ was established. The observed dependence of these values of $R_a - 1$ as a function of trap height was an extremely good match to that expected for a dipole field in the door cavity. The best-fit values of the parameters additionally favored a small (consistent with zero) separation arising from quadrupole fields that are slightly different for the two \mathbf{B}_0 field polarities. This overall scenario is also consistent (in both sign and magnitude) with the observation of a small difference in the value of $R_a - 1$ for the two field directions at which the neutron spin-depolarization rate was minimised.

Corrections for these additional fields, when calculated for the data-taking bottle, have the effect of increasing the measured EDM by $(1.10 \pm 0.80) \times 10^{-26}$ e cm, to yield a final value from this approach of

$$d_n = (+0.6 \pm 1.5 \text{ (stat)} \pm 0.8 \text{ (syst)}) \times 10^{-26} \text{ e cm}.$$

In this analysis, the systematic uncertainty is normally rather than uniformly distributed, and so the result may be interpreted as an upper limit on the magnitude of d_n of 3.0×10^{-26} e cm (90% CL).

V. DISCUSSION OF SYSTEMATIC EFFECTS

The systematic errors arising via the geometric phase coming from the combined action of $\mathbf{v} \times \mathbf{E}$ and \mathbf{B}_0 inhomogeneities have been described in Section IV. Further to these we consider other systematic effects, beginning with the usual first-order $\mathbf{v} \times \mathbf{E}$ effects.

If the UCN have a net translational motion, any perpendicular component of the electric field will be seen in their rest frame as a combination of electric and magnetic fields. During the 130 s Ramsey measurement period, the UCN ensemble may warm slightly due to vibrations. This causes the center of mass to rise by up to 0.1 cm. If the volume-averaged angle between \mathbf{E} and \mathbf{B} is as high as 0.05 radians, the induced false EDM will be 0.5×10^{-27} e cm.

Effect	Shift	σ
Door cavity dipole	-11.0	4.5
Other dipole fields	0.0	6.0
$\mathbf{v} \times \mathbf{E}$ translational	0.0	0.5
$\mathbf{v} \times \mathbf{E}$ rotational	0.0	1.0
Second-order $\mathbf{v} \times \mathbf{E}$	0.0	0.02
ν_{Hg} light shift (geo phase)	3.5	0.8
ν_{Hg} light shift (direct)	0.0	0.2
Uncompensated B drift	0.0	2.4
Hg atom EDM	0.0	0.5
Electric forces	0.0	0.4
Leakage currents	0.0	0.1
AC fields	0.0	0.01
Total	-7.5	8.0

TABLE I: Summary of systematic errors and their uncertainties, in units of 10^{-27} e cm.

In a similar manner to the translational effect, any net rotational flow of the UCN in conjunction with a radial component of the electric field may lead to an induced EDM signal. However, any such flow of UCN is expected to be attenuated by wall collisions before the first Ramsey pulse is applied. We calculate that the maximum error to be expected from this source and from higher-order $\mathbf{v} \times \mathbf{E}$ effects is below 1×10^{-27} e cm.

Next, we consider light shifts [16, 17]. Any small component of the ^{204}Hg probe light in the direction of the magnetic field, as it passes through the precessing ^{199}Hg atoms, will induce a shift of the precession frequency and thereby change slightly the frequency ratio R_a without creating any geometric-phase EDM. Thus, an error will arise in the geometric-phase correction. A slight dependence of R_a on the incident light intensity was indeed found, with a magnitude consistent with expectation from theory. In the second analysis a correction for this effect was made to the data on a run-by-run basis prior to the geometric-phase fitting described in section III above. This correction caused a reduction of $(3.5 \pm 0.8) \times 10^{-27}$ e cm in the fitted EDM value.

Analysis of the data suggested a possible small correlation between the intensity of the mercury reading light and the value of the applied electric field. Through the light shift, this could directly create an EDM signal. However, to within its uncertainty, the dependence of R_a on the light intensity has been removed. The residual systematic uncertainty on the EDM from this source is 0.2×10^{-27} e cm.

There may also be residual effects from magnetic field fluctuations. For example, a dipole-like field B_d originating from the region of the HV feedthrough would be sensed by both neutrons and mercury, but with a difference given by $\delta B_d / B_d = 3\Delta h / r$ where $r \sim 55$ cm is the distance from the source of the field to the center of the bottle, and $\Delta h = 0.28$ cm is the difference in height of the centers of mass of the mercury and neutrons. Thus, fluctuations in B that are correlated with the HV can be

expected to be compensated up to a factor of about 70. In order to study this, the mercury and neutron channels were analysed independently. The neutrons yielded an EDM signal of $(17 \pm 4) \times 10^{-26}$ e cm; the mercury, once the geometric-phase contribution (as calculated from the average $R_a - 1$ at which the data were taken) was subtracted, yielded $(-3.9 \pm 0.8) \times 10^{-26}$ e cm. These results are consistent with a common source of magnetic fluctuations correlated with the HV. We therefore expect the mercury compensation to shield us from this systematic effect to a level of $17 \times 10^{-26} / 70 = 2.4 \times 10^{-27}$ e cm.

As noted above, magnetic contaminants below the level of 1 nT cannot be ruled out. A Monte Carlo simulation of a dipole below the storage volume, incorporated within the mercury door mechanism, at a level that would produce a 1 nT field 1 cm above the surface yielded a possible residual false EDM of 6×10^{-27} e cm.

Any EDM of the mercury itself would affect the ratio R_a , and would thus contribute to a false EDM signal. However, the EDM of ^{199}Hg has been shown to be less than 0.21×10^{-27} e cm [6], corresponding to a limit of 0.81×10^{-27} e cm for a false nEDM signal from this source.

Another possible source of systematic error arises from electrostatic forces, which may move the electrodes slightly. In conjunction with a magnetic field gradient, an HV-dependent shift in the ratio would then appear. This was sought by looking for an EDM-like signal but with a frequency shift proportional to $|\mathbf{E}|$ instead of \mathbf{E} . The $|\mathbf{E}|$ signal was consistent with zero, with an uncertainty of 4×10^{-26} e cm. If the HV magnitudes were slightly different for the two signs of \mathbf{E} , this effect would generate a false EDM signal. Study of the measured HV and in particular of the charging currents show that the HV magnitude was the same for both polarities to within about 1%. This systematic uncertainty is therefore 0.4×10^{-27} e cm.

Analysis of the EDM as a function of leakage current shows no measurable effect. Leakage currents are typically of order 1 nA. If this current were to travel 10 cm azimuthally around the bottle, the resultant \mathbf{B} field would result in an apparent EDM of 0.1×10^{-27} e cm.

AC fields are another possible cause of concern. There is no differential ripple visible on the HV at the level of a few volts. Sampling is done at 5 Hz with a bandwidth of 20 kHz, so any substantial ripple at 50 Hz would show up as beats. It is certainly safe to say that there is no 50 Hz ripple at the level of 50 V, which would give a false EDM of 0.01×10^{-27} e cm.

Low-frequency AC fields were sought by means of a pickup coil in conjunction with a phase-sensitive detector. Shifts in R_a from this source at the level of 0.02 ppm could not be ruled out. Cancellations in the corresponding EDM signal from reversals of the electric and magnetic fields would reduce any net contribution to below the level of 0.01×10^{-27} e cm.

From the above considerations, it is clear that the total systematic uncertainty is dominated by the uncer-

tainty in shifts from the potential door-cavity dipole field and/or from extraeneous magnetic dipoles at a level undetectable with a fluxgate magnetometer. The others listed here are negligible in comparison.

VI. RESULTS AND CONCLUSION

The data set analysed here, which excludes data that have already been published [11], incorporates 545 measurement runs undertaken between the autumn of 1998 and the end of 2002. Two analyses have been carried out; neither obtained a result significantly different from zero. The results overall may be interpreted as an upper limit of $|d_n| < 3.0 \times 10^{-26} e \text{ cm}$ (90% CL) on the absolute value of the neutron EDM.

Acknowledgments

The authors are most grateful to N.F. Ramsey for many useful discussions and ideas; to Y. Chibane and

M. Chouder for their invaluable assistance in the early development of the mercury magnetometer; to I.A. Kilvington for vital engineering contributions; to the group of E.N. Fortson at the University of Washington, who made available information about the techniques that they had developed for magnetometry using atomic mercury; and to R. Baskin for computer simulation work. The experiments would of course not have been possible at all without the cooperation of, and generous provision of neutron facilities by, the ILL itself. This work has been funded by a grant from the UK Particle Physics and Astronomy Research Council (PPARC). Work at the University of Sussex was also supported by a grant from the UK Joint Infrastructure Fund. Support from the RFFI, via Grant No.03-02-17305, is gratefully acknowledged by S.N.I.

- [1] X.-G. He, B. McKellar, and S. Pakvasa, Phys. Rev. Lett. **61**, 1267 (1988).
- [2] J. Ellis and R. Flores, Phys. Lett. B **377**, 83 (1996).
- [3] M. Pospelov and A. Ritz, Annals of Physics **318**, 119 (2005); hep-ph/0504231.
- [4] S. Abel and O. Lebedev, JHEP **0601**, 133 (2006); hep-ph/0508135.
- [5] R. Peccei and H. Quinn, Phys. Rev. Lett. **38**, 1440 (1977).
- [6] M. Romalis, W. Griffith, and E. Fortson (2001).
- [7] B. Regan, E. Commins, C. Smidt, and D. DeMille, Phys. Rev. Lett. **88**, 071805 (2002).
- [8] O. Lebedev, K. Olive, M. Pospelov, and A. Ritz, Phys. Rev. D **70**, 016003 (2004).
- [9] S. Barr, Int. J. Mod. Phys. A **8**, 209 (1993).
- [10] N. Ramsey, in *Proc. XIV Int. Conf. Atomic Physics* (AIP, New York, 1994), p. 3.
- [11] P. Harris, C. Baker, K. Green, et al., Phys. Rev. Lett. **82**, 904 (1999).
- [12] K. Green, P. Harris, P. Iaydjiev, et al., Nucl. Instr. Meth. A **404**, 381 (1998).
- [13] J. Pendlebury et al., Phys. Rev. A **70**, 032102 (2004).
- [14] S. Lamoreaux and R. Golub, Phys. Rev. A **71**, 032104 (2005); nucl-ex/0407005.
- [15] P. Harris and J. Pendlebury, Phys. Rev. A **73**, 014101 (2006); physics/0510134.
- [16] C. Cohen-Tannoudji and J. Dupont-Roc, Phys. Rev. A **5**, 968 (1972).
- [17] A. Corney, *Atomic and Laser Spectroscopy* (Oxford University Press, 1968).